

***Design and analysis of
oxidation tests to inform
FeCrAl ATF severe
accident models
(M3NT-18OR020205041)***

***Prepared for
U.S. Department of Energy
Advanced Fuel Campaign
Kevin R. Robb
Michael Howell
Larry J. Ott
Oak Ridge National Laboratory
July 2018
M3NT-18OR020205041
ORNL/SPR-2018/893***

DOCUMENT AVAILABILITY

Reports produced after January 1, 1996, are generally available free via US Department of Energy (DOE) SciTech Connect.

Website <http://www.osti.gov/>

Reports produced before January 1, 1996, may be purchased by members of the public from the following source:

National Technical Information Service
5285 Port Royal Road
Springfield, VA 22161
Telephone 703-605-6000 (1-800-553-6847)
TDD 703-487-4639
Fax 703-605-6900
E-mail info@ntis.gov
Website <http://www.ntis.gov/help/ordermethods.aspx>

Reports are available to DOE employees, DOE contractors, Energy Technology Data Exchange representatives, and International Nuclear Information System representatives from the following source:

Office of Scientific and Technical Information
PO Box 62
Oak Ridge, TN 37831
Telephone 865-576-8401
Fax 865-576-5728
E-mail reports@osti.gov
Website <http://www.osti.gov/contact.html>

This report was prepared as an account of work sponsored by an agency of the United States Government. Neither the United States Government nor any agency thereof, nor any of their employees, makes any warranty, express or implied, or assumes any legal liability or responsibility for the accuracy, completeness, or usefulness of any information, apparatus, product, or process disclosed, or represents that its use would not infringe privately owned rights. Reference herein to any specific commercial product, process, or service by trade name, trademark, manufacturer, or otherwise, does not necessarily constitute or imply its endorsement, recommendation, or favoring by the United States Government or any agency thereof. The views and opinions of authors expressed herein do not necessarily state or reflect those of the United States Government or any agency thereof.

Nuclear Technology Research and Development–Advanced Fuels Campaign

**Parametric and Experimentally Informed BWR Severe Accident Analysis Using FeCrAl
(M3NT-18OR020205041)**

Kevin R. Robb
Michael Howell
Larry J. Ott

Date Published:
July 2018

Prepared by
OAK RIDGE NATIONAL LABORATORY
Oak Ridge, TN 37831-6283
managed by
UT-BATTELLE, LLC
for the
US DEPARTMENT OF ENERGY
under contract DE-AC05-00OR22725

CONTENTS

	Page
LIST OF FIGURES	v
LIST OF TABLES	vii
ACRONYMS and ABBREVIATIONS	ix
ACKNOWLEDGMENTS	xi
ABSTRACT.....	xiii
1. INTRODUCTION	1
2. FeCrAl oxidation testing.....	2
2.1 INTRODUCTION	2
2.1.1 Common Test Procedures	2
2.2 QUENCH-STYLE Oxidation TEST SERIES	2
2.2.1 Test Procedure	3
2.2.2 Test Results.....	4
2.3 SBO STYLE OXIDATION TEST SERIES	7
2.3.1 Test Procedure	7
2.3.2 Test Results.....	8
2.4 OXIDATION KINETICS EVALUATION	10
2.5 BREAKAWAY OXIDATION ONSET DISCUSSION	14
3. FECRAL MATERIAL INTERACTION TESTS.....	16
3.1 Test setup and conduct.....	16
3.2 Test Series and Results	17
3.3 Results Discussion	19
4. SUMMARY.....	20
5. REFERENCES	21
Appendix A: B136Y OXIDATION TEST DATA	1

LIST OF FIGURES

	Page
Figure 1. Heating segment illustration for QUENCH-style oxidation tests.....	3
Figure 2. Test endpoints for QUENCH-style oxidation tests.	4
Figure 3. Specific mass change (mg/cm ²) for QUENCH-style oxidation tests.	6
Figure 4. Posttest images of QUENCH-style tests.....	6
Figure 5. Heating segment illustration for SBO-style oxidation tests.....	8
Figure 6. Posttest images of SBO-style tests.	9
Figure 7. Predicted vs. measured mass gain, using Eq. 1.	12
Figure 8. Predicted vs. measured mass gain, using 3 × Eq. 1.	12
Figure 9. Predicted vs. measured mass gain, using 5× Eq. 1.	13
Figure 10. Predicted vs. measured mass gain, using 10× Eq. 1.	13
Figure 11. HTF tests with B136Y indicating temperature history and whether extensive attack occurred.	15

LIST OF TABLES

	Page
Table 1. Steam velocity vs. temperature in the HTF.....	2
Table 2. Test segments: QUENCH-style oxidation tests	3
Table 3. Test number and maximum furnace temperature—QUENCH-style oxidation tests.....	3
Table 4. Test result summary—QUENCH-style tests	5
Table 5. Test segments—SBO-style oxidation tests.....	8
Table 6. Test result summary—SBO-style tests	9
Table 7. Measured and predicted oxidation mass change of B136Y	11
Table 8. Summary of FeCrAl cladding ramp oxidation testing in HTF with 200 mL/h steam flow	15

ACRONYMS AND ABBREVIATIONS

ATF	accident-tolerant fuel
BWR	boiling water reactor
DOE	US Department of Energy
FeCrAl	iron-chromium-aluminum alloy
HTF	high-temperature furnace
KIT	Karlsruhe Institute of Technology
ORNL	Oak Ridge National Laboratory
RMSD	root mean square deviation
RPV	reactor pressure vessel
SBO	station blackout

ACKNOWLEDGMENTS

This work was supported through the Advanced Fuels Campaign within the US Department of Energy Office of Nuclear Energy.

ABSTRACT

Iron-chromium-aluminum (FeCrAl) alloys are being considered as advanced fuel cladding concepts with enhanced accident tolerance. At high temperatures, FeCrAl alloys have slower oxidation kinetics and higher strength compared with zirconium-based alloys. FeCrAl could be used for fuel cladding and spacer or mixing vane grids in light water reactors and/or as channel box material in boiling water reactors (BWRs). There is a need to assess the potential gains afforded by the FeCrAl accident-tolerant-fuel (ATF) concept over the existing zirconium-based materials employed today.

To accurately assess the response of FeCrAl alloys under severe accident conditions, a number of FeCrAl properties and characteristics are required. These include thermophysical properties as well as burst characteristics, oxidation kinetics, possible eutectic interactions, and failure temperatures. These properties can vary among different FeCrAl alloys.

Oak Ridge National Laboratory has pursued refined values for the oxidation kinetics of the B136Y FeCrAl alloy (Fe-13Cr-6Al wt %). This investigation included oxidation tests with varying heating rates and end-point temperatures in a steam environment. The rate constant for the low-temperature oxidation kinetics was found to be higher than that for the commercial APMT FeCrAl alloy (Fe-21Cr-5Al-3Mo wt %). Compared with APMT, a 5 times higher rate constant best predicted the entire dataset (root mean square deviation). Based on tests following heating rates comparable with those the cladding would experience during a station blackout, the transition to higher oxidation kinetics occurs at approximately 1,500°C.

During a severe accident, materials interactions (e.g. eutectic formation and material dissolution) may occur between the range of materials comprising the reactor core. Interactions between FeCrAl and SS304H, Inconel®718, and B₄C were investigated experimentally in an inert environment. At temperatures below 1500°C, no substantial materials interaction was observed to occur. In contrast, at 1300°C, extensive interaction between SS304H and B₄C was observed. These results are largely consistent with similar tests conducted internationally.

1. INTRODUCTION

The US Department of Energy (DOE) Fuel Cycle Research and Development Advanced Fuels Campaign is leading the research, development, and demonstration of nuclear fuels with enhanced accident tolerance [1]. Accident-tolerant fuels (ATFs) are fuels and/or cladding that, in comparison with the standard uranium fuel–Zr-based alloy cladding system, can tolerate loss of active cooling in the core for a considerably longer time period while maintaining or improving the fuel performance during normal operations. Note that currently used uranium–Zr-based cladding fuel systems tolerate design-basis accidents (and anticipated operational occurrences and normal operation) as prescribed by the US Nuclear Regulatory Commission. There are three major potential approaches for the development of ATFs

1. improving fuel properties,
2. improving cladding properties to maintain core coolability and retain fission products, and
3. reducing the rate of reaction kinetics with steam to minimize enthalpy input and hydrogen generation.

A proposed ATF concept is based on iron-chromium-aluminum alloys (FeCrAl) [2]. With respect to enhancing accident tolerance, FeCrAl alloys have substantially slower oxidation kinetics compared with currently used zirconium alloys. During a severe accident, FeCrAl would tend to generate heat and hydrogen from oxidation at a slower rate compared with zirconium-based alloys.

This report documents an extension of previous efforts [3] to investigate the oxidation kinetics of the B136Y FeCrAl alloy. Much of the content from Section 2 of Ref. [3] is included in this report to provide context and for the convenience of the reader. The simulated conditions (Section 2.2) were designed to aid in planning and in pre- and posttest calculations for an upcoming QUENCH test at the Karlsruhe Institute of Technology (KIT) that will also use the B136Y alloy. An additional series of oxidation tests using the B136Y alloy were conducted at ORNL following temperature ramp rates based on previous station blackout simulations (Section 2.3). These tests provide insight into the cladding behavior during anticipated accident conditions. Using the test data, the oxidation kinetics (Section 2.4), and the temperature at which rapid attack of the cladding by steam is initiated (Section 2.5) are examined. The interaction of the B136Y alloy with other materials was investigated in Section 3. Findings and suggested future work are discussed in Section 4.

2. FECRAL OXIDATION TESTING

2.1 INTRODUCTION

The APMT FeCrAl alloy (Fe-21Cr-5Al-3Mo wt %) is a commercial alloy for which oxidation tests and the development of oxidation kinetics have been previously conducted [4]. However, development has been under way at ORNL to produce a material with properties suitable for nuclear reactor operations. For this application, the FeCrAl alloy Fe-13Cr-6Al (B136Y) is a first-generation alloy tested at ORNL that has more favorable irradiation properties than that of the commercial APMT alloy. B136Y will be used in a planned QUENCH test at KIT. Two series of oxidation tests in steam were performed with B136Y and are discussed in Sections 2.2 and 2.3. This is followed by a review of the test data with respect to oxidation kinetics (Section 2.4) and the onset temperature for rapid attack of the alloy by steam (Section 2.5).

2.1.1 Common Test Procedures

For both oxidation test series, tube segments of B136Y were exposed to a steam environment in ORNL's high-temperature furnace (HTF) [5]. Samples of B136Y tubing were taken from the same lot of tubing that will be used in the planned QUENCH test at KIT. The samples were approximately 9.51 mm OD and 12.62 mm long (see Appendix A for detailed measurements).

During the test, a cladding segment was first ramped from room temperature to 600°C under an argon atmosphere at a rate of 20°C/min. The sample was held at 600°C for one min. Following this test segment, the argon supply was shut off, steam was supplied to the test section, and the temperature was ramped at prescribed rates. Steam was supplied to the test section by injecting water into the lower portion of the preheat furnace at a constant rate of 0.0556 g/s (200 mL/h). The area averaged steam velocity, based on the geometry of the furnace, is provided in Table 1. The tests were concluded by turning off power to the furnace, turning off the steam supply, and supplying argon to the test section. All tests were performed at atmospheric pressure. Note that the measured, controlled, and reported temperatures are based on furnace thermocouples and are not measurements of actual sample temperatures.

Table 1. Steam velocity vs. temperature in the HTF

Temp. (°C)	Steam velocity(cm/s)
1,500	56.7
1,400	53.5
1,300	50.3
1,200	47.1
1,100	43.9
1,000	40.7
900	37.5
800	34.3
700	31.1
600	27.9

2.2 QUENCH-STYLE OXIDATION TEST SERIES

The first series of tests were conducted to aid in planning the future FeCrAl QUENCH test, provide insight into the anticipated behavior of the cladding during the QUENCH test, and help refine the oxidation kinetics for pre- and post-QUENCH test simulations.

2.2.1 Test Procedure

Within the capabilities of the HTF, samples were exposed to conditions (i.e., temperature vs. time with flowing steam environment) approximating those of the QUENCH-15 test (i.e., same as those planned for the FeCrAl QUENCH test). The various test segments are described in Table 2 and illustrated in Figure 1. Several tests were performed with various stopping points. The tests and temperature at which the tests were stopped are illustrated in Figure 2 and summarized in Table 3. Also included in Figure 1 and Figure 2 is data from the QUENCH-15 test for the 950 mm elevation (digitized from Fig. 19, red curve, Ref. [6]). Additional test details are provided in Appendix A. A variation of the test conditions was also explored in tests 18 and 21 which extended the hold time of segment 2 to 150.9 min. This was conducted to investigate the effect of the “pre-oxidation” phase of the QUENCH tests on the FeCrAl alloy.

Table 2. Test segments: QUENCH-style oxidation tests

Segment	Ramp rate (°C/min)	Target temp. (°C)	Hold time at target temp. (min)
1	20	600	1
2	12	1,200	50.3
3	11.1	1,400–1,500	1

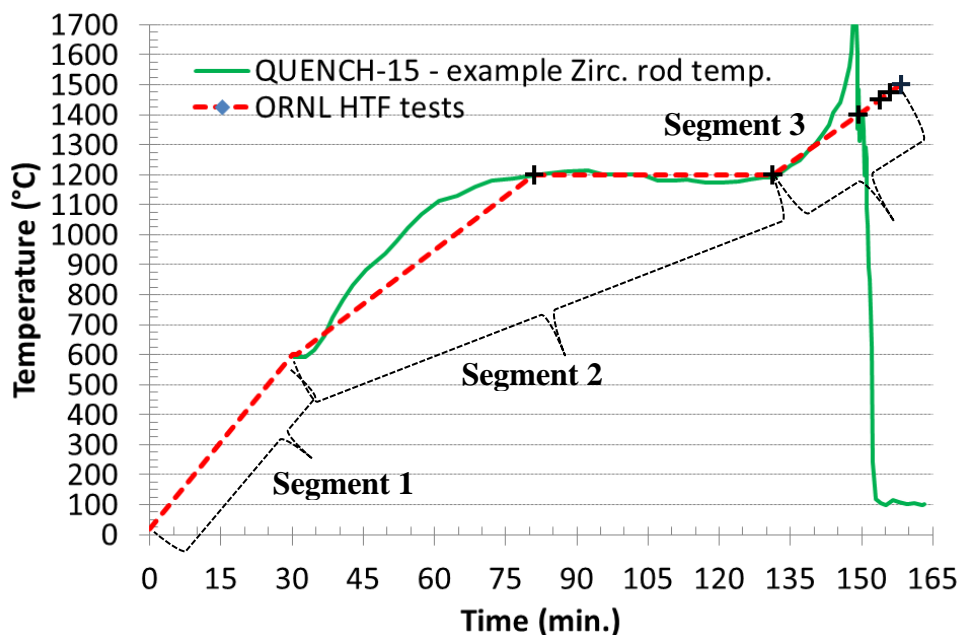


Figure 1. Heating segment illustration for QUENCH-style oxidation tests.

Table 3. Test number and maximum furnace temperature—QUENCH-style oxidation tests

Test	Maximum furnace temp. (°C)	Notes
------	----------------------------------	-------

22	1,050	Only 1 min hold after reaching 1,050°C
1	1,200	Only 1 min hold after reaching 1,200°C
2	1,200	
3	1,400	
19	1,400	Repeat of test 3
20	1,400	Repeat of test 3
15	1,450	
16	1,475	
4	1,500	
18	1,200	Similar to test 2; however, the hold time at 1,200°C was 150.9 min (3 times the duration of other tests).
21	1,200	Repeat of test 18

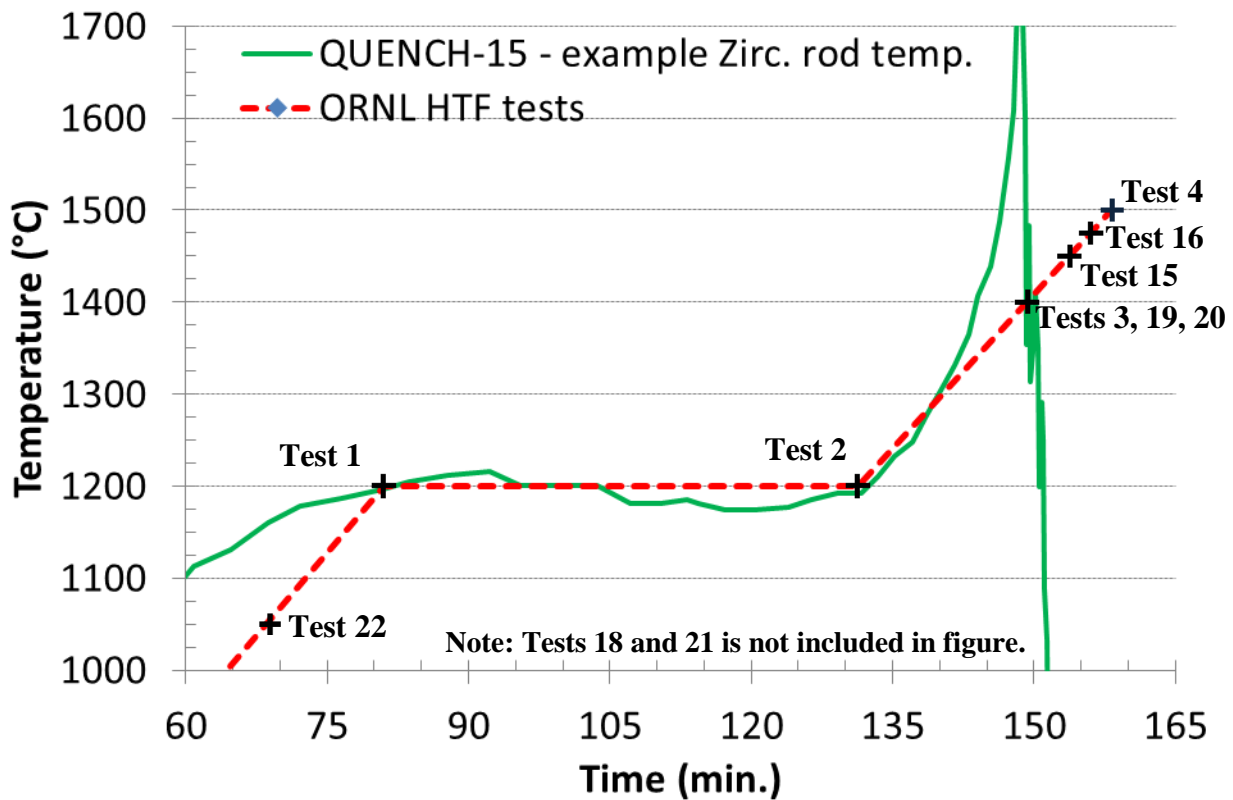


Figure 2. Test endpoints for QUENCH-style oxidation tests.

2.2.2 Test Results

Changes in sample mass pre- and posttest are noted in Table 4 and Figure 3 for the eleven tests conducted. Posttest images of selected tests are provided in Figure 4. Tests conducted at lower temperatures were visually similar to the nontested cladding.

The high specific mass changes noted for test 16, 59.3 mg/cm², and test 4, 62.3 mg/cm², indicate substantial attack and degradation of the cladding. If all the aluminum in the sample is assumed to oxidize forming Al₂O₃, the specific mass gain would be approximately 7.0 mg/cm². The specific mass gains for tests 16 and 4 are much higher than this, indicating oxidation of other alloy constituents. Complete oxidation of the sample into Al₂O₃, Fe₃O₄, and Cr₂O₃ (assuming Fe-13Cr-6Al) would result in a weight

gain of 55.3 mg/cm². The experimental data suggest complete oxidation of the cladding for tests 16 and 4 and the possible formation of other oxides. The cladding degradation for tests 16 and 4 is visually evident in Figure 4. Tests conducted at lower temperatures, 1,450°C and below, have relatively low mass gains (i.e., 1.1% or less of the initial sample mass) and remained intact.

Tests 1, 2, and 18 and 21 show the impact of the pre-oxidation phase of the QUENCH test. Only modest oxidation occurs at 1,200°C.

Comparing the specific mass change results shown in Figure 3, indicates there is variation between tests. A clear trend between the test conditions and specific mass change is not evident. The mass gains (i.e. less than 1.1% of the sample mass) and the differences between mass gains are small (i.e., the discrepancies are between small numbers). Possible causes for the discrepancies could be attributed to differences in sample edge conditions (i.e., a small burr or other imperfection), variation in test conditions, and/or minor mass loss during sample handling. Additional repeatability and refinement of the oxidation testing setup is recommended for future work.

Following the temperature ramp conditions of QUENCH-15 and neglecting the rapid exothermic reaction of Zircaloy during the QUENCH-15 test, the HTF tests with B136Y indicate the cladding will remain intact for the anticipated peak temperatures of 1,375-1,400°C in the planned FeCrAl QUENCH test.

Table 4. Test result summary—QUENCH-style tests

Test	Max furnace temp. (°C)	Calc. area (cm ²)	Pre- and posttest mass gain (mg)	Pre- and posttest specific mass change (mg/cm ²)
22	1,050	7.438	2.98	0.401
1	1,200	7.468	1.56	0.209
2	1,200	7.455	1.82	0.244
18 ^a	1,200	7.440	2.89	0.388
21 ^a	1,200	7.085	4.70	0.663
3	1,400	7.463	6.60	0.884
19	1,400	8.830	12.96	1.468
20	1,400	7.466	5.38	0.721
15	1,450	7.449	4.01	0.538
16	1,475	7.456	442.28	59.32
4	1,500	7.463	464.68	62.26

^aTest was held at 1,200°C for 150.9 min.

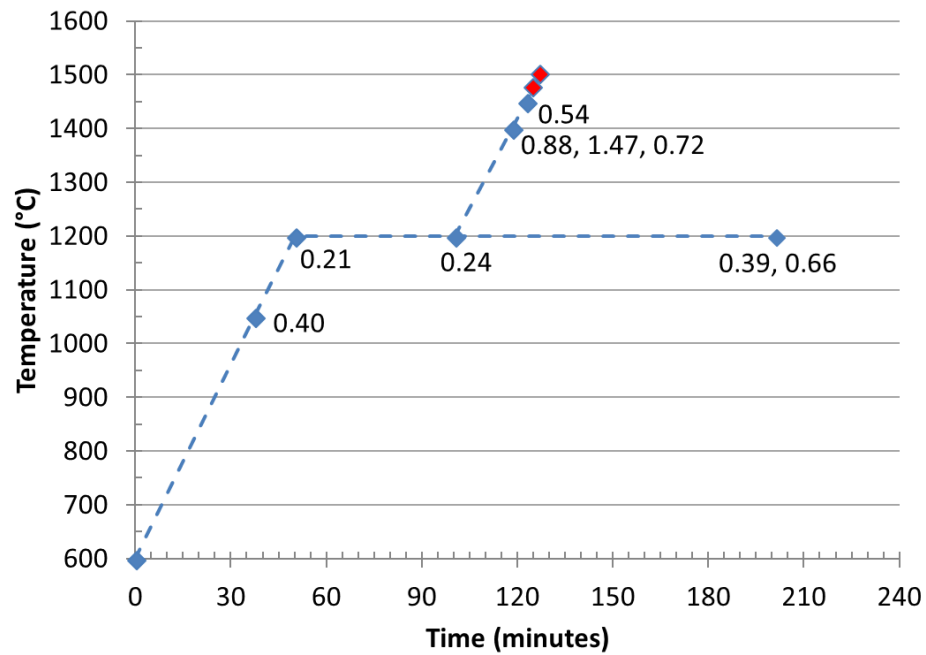


Figure 3. Specific mass change (mg/cm²) for QUENCH-style oxidation tests.

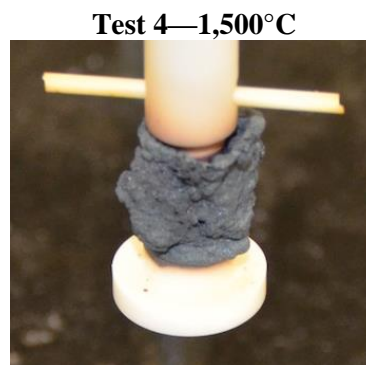
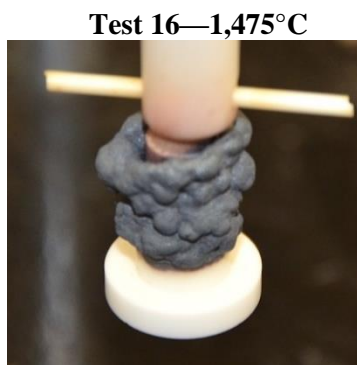
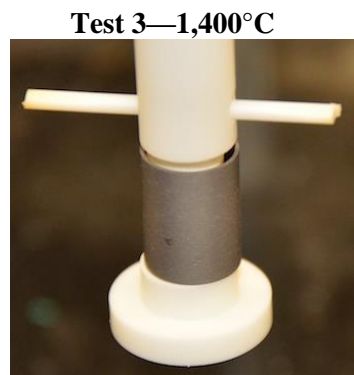


Figure 4. Posttest images of QUENCH-style tests.

2.3 SBO STYLE OXIDATION TEST SERIES

A second set of oxidation tests were conducted based on ramp rates derived from previous MELCOR simulations of boiling water reactor (BWR) station blackout (SBO) scenarios [7]. The objective of the tests was to observe the cladding response during prototypic temperature ramp rates (i.e., more prototypic compared with isothermal tests, past ramps, or the QUENCH-15 ramp sequence). The test data is used in the assessment of the oxidation kinetics for B136Y (see Section 2.4). Also, the tests provide some confirmation of the anticipated cladding performance during simulated and actual severe accident conditions. The tests however did not match the steam flow rate or pressure of the predicted SBO simulations. The cladding was “beginning of life” in that the cladding was neither pre-oxidized in prototypic BWR conditions nor previously irradiated.

2.3.1 Test Procedure

Three simplified temperature histories, based on previous SBO analyses, were applied to the HTF. Each history included three segments. Same as the QUENCH-style tests, the first segment was a ramp at 20°C/min to 600°C in an argon atmosphere with a 1 min hold at 600°C. The second and third segments, where applicable, are provided in Table 5. The tests were stopped after segment 2 or 3.

Table 5. Test segments—SBO-style oxidation tests

Test	Segment 2			Segment 3		
	Ramp rate (°C/min)	Target Temp. (°C)	Hold time at target temp. (min)	Ramp rate (°C/min)	Target temp. (°C)	Hold time at target temp. (min)
7	16.67	1412	1	NA ^a	NA	NA
8	16.67	1412	1	4.17	1500	1
9	7.41	1182	1	NA ^a	NA	NA
10	7.41	1182	1	1.81	1500	1
17	7.41	1182	1	1.81	1550	1
23	7.41	1182	1	1.81	1550	1
11	5.70	1108	1	NA ^a	NA	NA
12	5.70	1108	1	1.57	1500	1

^aNot applicable; test stopped after Segment 2.

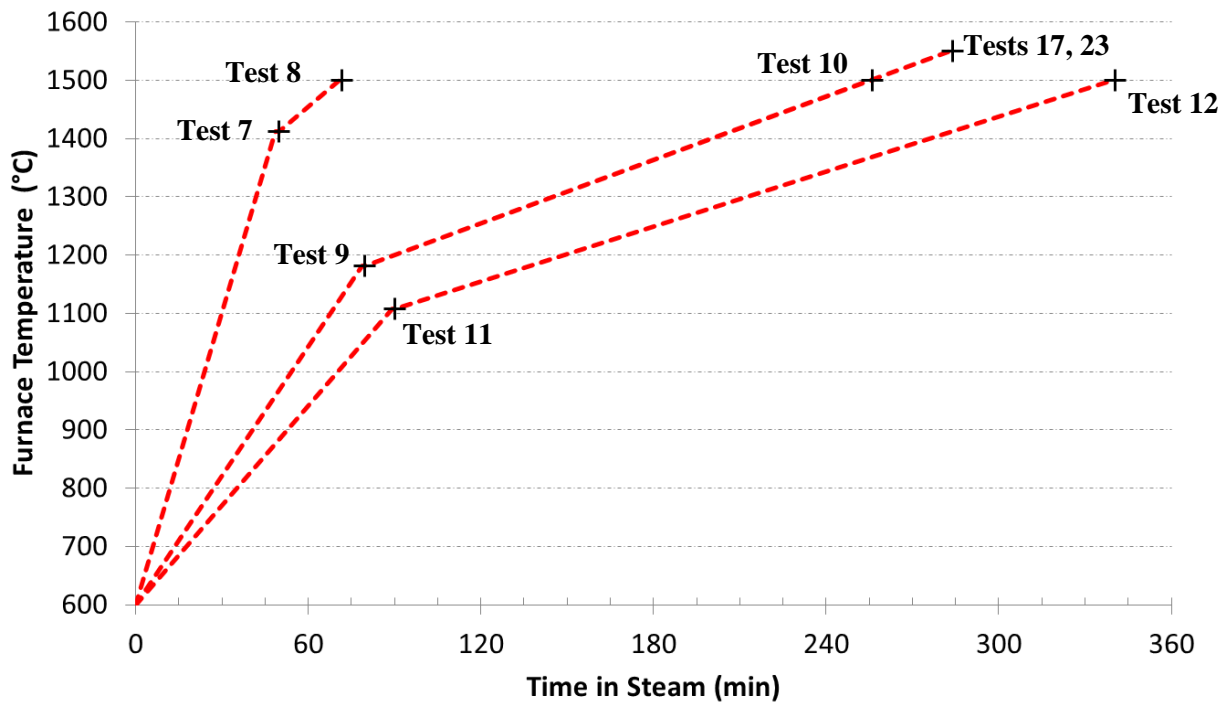


Figure 5. Heating segment illustration for SBO-style oxidation tests.

2.3.2 Test Results

Changes in sample mass pre- and posttest are noted in Table 6 for the seven tests conducted. Posttest images of select tests are provided in Figure 6.

In contrast to the QUENCH-style tests (see Section 2.2), all three tests conducted to 1,500°C did not suffer from substantial attack.

Two tests were conducted to a maximum temperature of 1,550°C (i.e. tests 17 and 23). The posttest appearance of test 17 is unique from any previous B136Y high-temperature steam oxidation test (see Section 2.2.2 and Ref. [9]). The cladding remained “intact,” with no gross signs of melting or change in

geometry. However, the pre- and posttest mass measurements indicate a slight loss of mass. In contrast, test 23 experienced substantial attack and degradation of the cladding.

Further analysis and testing are required to understand the cladding response at such high temperatures. These results suggest the cladding might stay intact up to 1,500°C under temperature ramp rates predicted for SBO accidents.

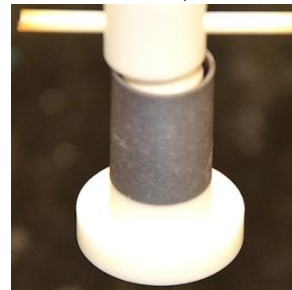
Table 6. Test result summary—SBO-style tests

Test	Max furnace temp. (°C)	Calc. area (cm²)	Pre- and posttest mass gain (mg)	Pre- and posttest specific mass change (mg/cm²)
7	1412	7.444	3.04	0.408
8	1500	7.441	5.49	0.738
9	1182	7.452	1.07	0.144
10	1500	7.446	7.33	0.984
17	1550	7.448	-0.4	-0.054
23	1550	7.463	848.95	113.75
11	1108	7.447	1.9	0.255
12	1500	7.435	7.54	1.014

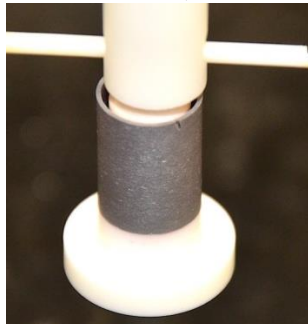
Test 9—1,182°C



Test 10—1,500°C



Test 12—1,500°C



Test 17—1,550°C



Figure 6. Posttest images of SBO-style tests.

2.4 OXIDATION KINETICS EVALUATION

In previous simulation efforts [7], the parabolic oxidation kinetics before the onset of rapid attack were modeled using Eqs. 1 and 2. These kinetics are those previously determined for APMT [4]. After the onset of rapid attack, the default parabolic oxidation kinetics for stainless steel in MELCOR were used [8]. The transition temperature specified for the onset of rapid attack was assumed to be 1,773 K (1,500°C).

$$K(T) = 230 \cdot e^{(-41376.0/T)} \quad \text{for } T \leq 1,773 \text{ K} , \quad (1)$$

and

$$K(T) = (2.42 \cdot 10^9) \cdot e^{(-42400.0/T)} \quad \text{for } T > 1,773 \text{ K} , \quad (2)$$

where

T = temperature (Kelvin),

$K(T)$ = reaction rate constant with respect to metal reacted ($\text{kg}^2/(\text{m}^4 \text{ s})$).

Numerically, the mass of reacted metal is evaluated using Eq. 3. To convert metal that has reacted to the oxide produced, it is assumed that aluminum is reacting to form Al_2O_3 for the low-temperature oxidation regime (before Al_2O_3 scale fails) (see Eq. 4). The mass gain can then be determined by the difference between the mass of the oxide formed and the mass of the reacted metal.

$$W_{\text{metal}}^{n+1} = \sqrt{\left((W_{\text{metal}}^n)^2 + K(T^n) \cdot (\Delta t) \right)} , \quad (3)$$

and

$$W_{\text{oxide}} = W_{\text{metal}} \cdot \left(\frac{101.964}{2 \cdot 26.982} \right) = W_{\text{metal}} \cdot 1.8895 , \quad (4)$$

where

T = temperature (Kelvin),

$K(T)$ = rate constant with respect to metal reacted $\text{kg}^2/(\text{m}^4 \text{ s})$,

Δt = time step size (s),

n = the previous time step,

$^{n+1}$ = the current time step,

W_{metal} = metal mass reacted (kg),

W_{oxide} = oxide mass produced (kg).

Based on these relations, the predicted specific mass change for the tests, using the low-temperature oxidation kinetics, is summarized in Table 7 and plotted in Figure 7. Tests 16, 4, and 23 are included and noted in red; however, these three tests experienced substantial attack for which the low-temperature oxidation kinetic is not applicable. Test 17, which was a unique test result with slight mass loss, is also included and noted in red. Two additional test data points are included from previous oxidation testing with B136Y [9]. One data point is from a test in the HTF in which the cladding was ramped from room temperature to 1,400°C in 90 min, with a flowing steam environment of 0.0556 g/s (200 mL/h) for temperatures above 600°C. The other data point is from a test performed in a thermogravimetric analysis device (TGA) that was ramped to 1,480°C at 5°C/min with a steam environment flow at approximately 1 cm/s.

Using Eq. 1, the mass gain is underpredicted for all tests that did not suffer from extensive attack. The leading coefficient in Eq. 1 was increased by factors of 3, 5, and 10 \times . The specific mass changes predicted using the increased oxidation kinetics are provided in Table 7 and plotted in Figure 8 and Figure 10.

By increasing the oxidation rate constant by a factor of 3, the predicted specific mass gain for tests 10 and 12, both SBO-style tests to 1,500°C, align well with the measured data (see Figure 8). However, the rest of the test data is still underpredicted.

When the oxidation rate constant is increased by a factor of 10, the predicted specific mass gain for the tests conducted to higher temperatures (i.e., $\geq 1,450^\circ\text{C}$) are overpredicted while the lower temperature tests are still slightly underpredicted, Figure 10.

The root mean square deviation (RMSD) of the predicted specific mass changes is 0.503, 0.416, 0.394, and 0.449 for multipliers of Eq. 1 of 1, 3, 5, and 10, respectively (for the 17 tests that did not experience substantial attack). The minimum RMSD was achieved with a multiplier of 5.

Table 7. Measured and predicted oxidation mass change of B136Y

Series	Test	Max furnace temp. ($^\circ\text{C}$)	Specific mass change (mg/cm^2)				
			Measured	Predicted			
				Eq. 1	$3 \times \text{Eq. 1}$	$5 \times \text{Eq. 1}$	$10 \times \text{Eq. 1}$
QUENCH	22	1050	0.401	0.004	0.006	0.008	0.011
	1	1200	0.209	0.019	0.032	0.042	0.059
	2	1200	0.244	0.061	0.106	0.137	0.194
	18	1200	0.388	0.103	0.179	0.231	0.327
	21	1200	0.663	0.103	0.179	0.231	0.327
	3	1400	0.884	0.129	0.223	0.288	0.408
	19	1400	1.468	0.129	0.223	0.288	0.408
	20	1400	0.721	0.129	0.223	0.288	0.408
	15	1450	0.538	0.178	0.309	0.399	0.564
	<i>16</i>	<i>1475</i>	<i>59.32</i>	<i>0.211</i>	<i>0.366</i>	<i>0.472</i>	<i>0.668</i>
	<i>4</i>	<i>1500</i>	<i>62.26</i>	<i>0.250</i>	<i>0.433</i>	<i>0.559</i>	<i>0.790</i>
SBO	7	1412	0.408	0.106	0.184	0.238	0.337
	8	1500	0.738	0.343	0.594	0.767	1.085
	9	1182	0.144	0.019	0.033	0.043	0.061
	10	1500	0.984	0.562	0.973	1.256	1.776
	<i>17</i>	<i>1550</i>	<i>-0.054</i>	<i>0.796</i>	<i>1.379</i>	<i>1.781</i>	<i>2.518</i>
	<i>23</i>	<i>1550</i>	<i>113.8</i>	<i>0.796</i>	<i>1.379</i>	<i>1.781</i>	<i>2.518</i>
	11	1108	0.255	0.010	0.017	0.021	0.030
	12	1500	1.014	0.602	1.043	1.347	1.905
Ref. [9] HTF	-	1400	0.32	0.090	0.156	0.201	0.284
Ref. [9] TGA	-	1480	0.66	0.290	0.502	0.648	0.917

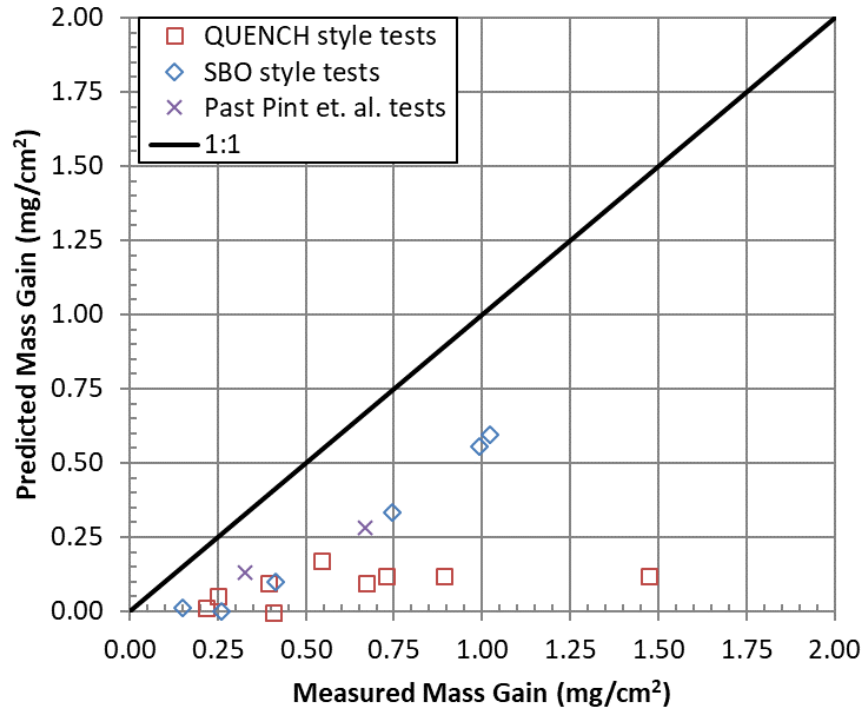


Figure 7. Predicted vs. measured mass gain, using Eq. 1.

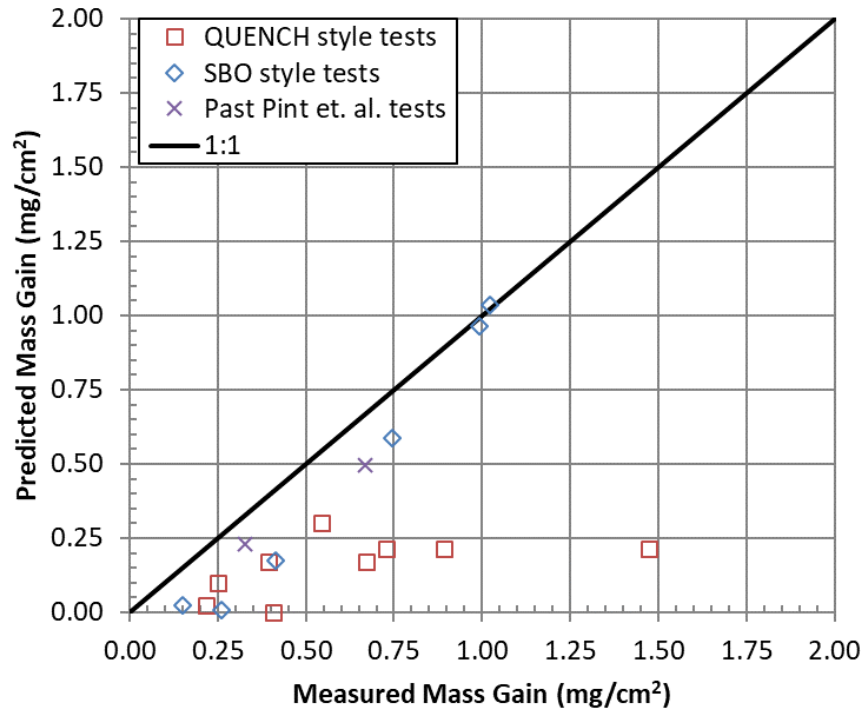


Figure 8. Predicted vs. measured mass gain, using $3 \times$ Eq. 1.

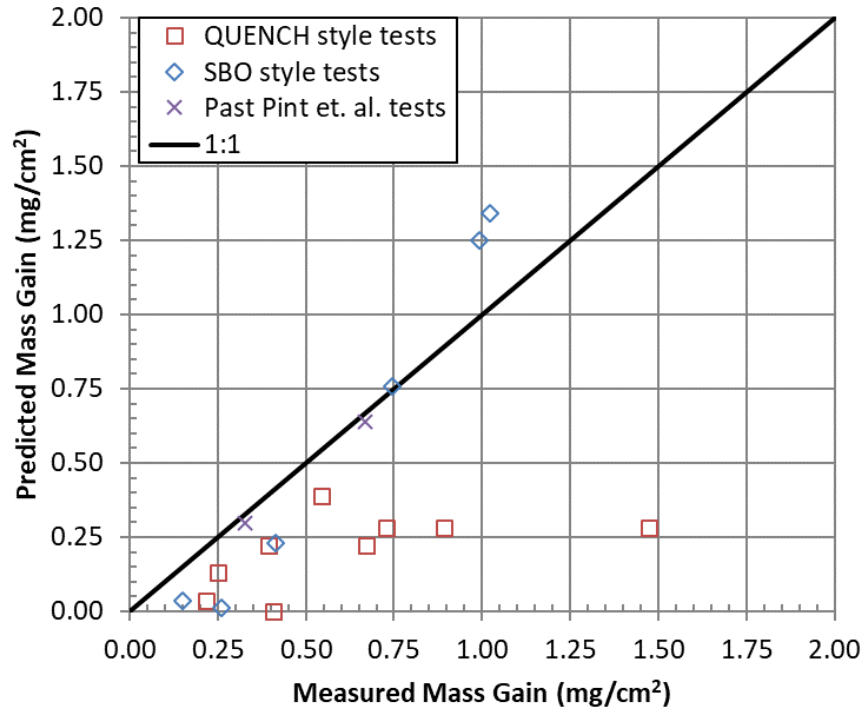


Figure 9. Predicted vs. measured mass gain, using 5× Eq. 1.

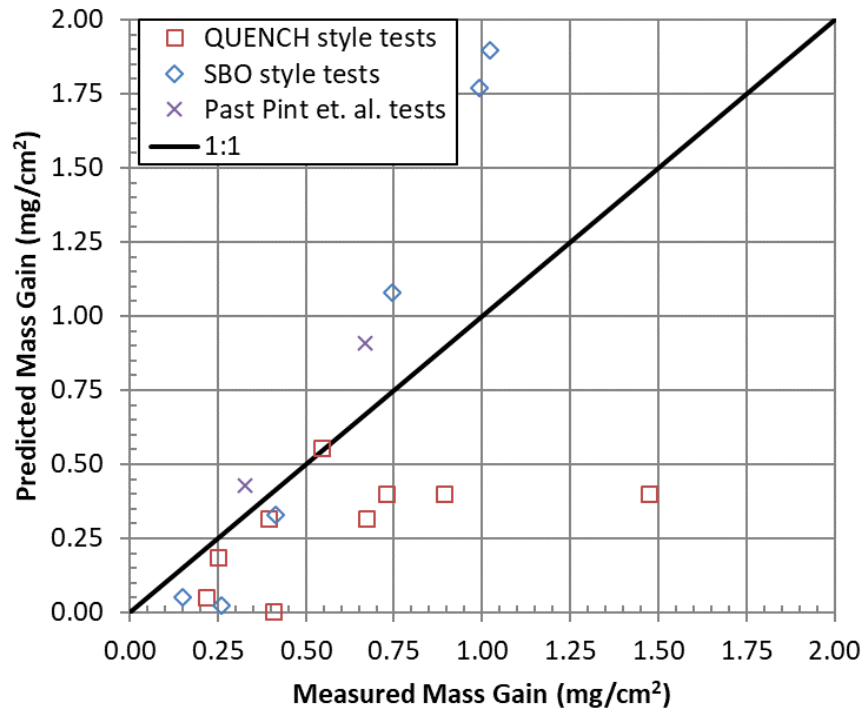


Figure 10. Predicted vs. measured mass gain, using 10× Eq. 1.

2.5 BREAKAWAY OXIDATION ONSET DISCUSSION

At a high enough temperature the cladding suffers from rapid and extensive attack by steam. Evidence of extensive oxidation and melting has been observed in previous tests [9], as well as in the current work (see Sections 2.2.2 and 2.3.2). Figure 11 and Table 8 summarize the B136Y oxidation tests and whether extensive attack was observed. All tests were conducted in the HTF and had 0.0556 g/s (200 mL/h) steam flow rate. In the current study, the B136Y cladding was extensively attacked at 1,475°C and at 1,500°C during the QUENCH-style tests and during a previous test to 1,500°C [9]. However, the cladding reached 1,500°C in all three reactor SBO-style oxidation tests without extensive attack.

Previous simulations [7] used 1,500°C as the transition between low-temperature oxidation kinetics and rapid oxidation at higher temperatures based on the test data for the APMT alloy. The test data for B136Y, a more representative alloy for nuclear reactor applications than APMT, continues to support this transition temperature for SBO-type scenarios.

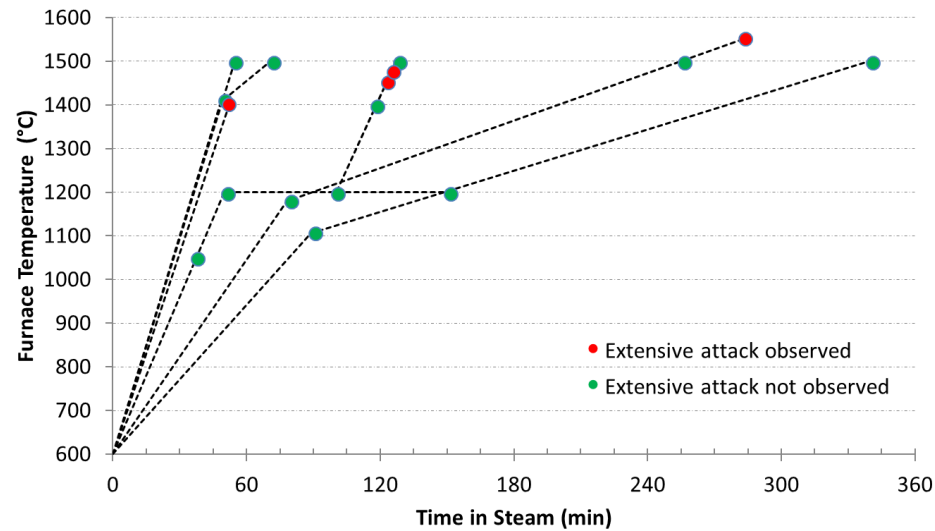


Figure 11. HTF tests with B136Y indicating temperature history and whether extensive attack occurred.

Table 8. Summary of FeCrAl cladding ramp oxidation testing in HTF with 200 mL/h steam flow

Reference	Test number	Alloy	Ramp rate at high temp.(°C/min)	Time above600°C & steam(min)	Melting or accelerated oxidation (°C)					
					1400	1450	1475	1500	1550	1600 1700
Ref [9]	-	B136Y	15.3, 16.4	52.2, 54.7	✓			X		
	7	B136Y	16.67	49.7	✓ ^a					
Current work	3, 15, 16, 4, 19, 20	B136Y	11.1	119.3-128.3	✓	✓	X	X		
	8	B136Y	4.17	71.8				✓		
	10, 17, 23	B136Y	1.81	256.1, 283.9				✓	X ^b	
	12	B136Y	1.57	340.6				✓		
Additional tests										
Ref [9]	-	APM	15.3-19	52-59	✓			✓		X X
	-	C135M	15.3, 16.4	52.2, 54.7	X			X		

✓ = Melting or accelerated oxidation did not occur.

X = Melting or accelerated oxidation occurred.

^aActually went to 1,412°C.

^bExtensive attack seen in test 23 and a unique result observed in test 17 where sample appeared intact but with slight mass loss

3. FECRAL MATERIAL INTERACTION TESTS

Beyond the uranium dioxide fuel and cladding, light water reactors contain a few different materials in the core region. These materials include control materials (e.g. Ag-In-Cd and B₄C), burnable absorbers (e.g. Gd), various hardware (i.e. sheaths, grids, springs) that can consist of 304 stainless steel and/or INCONEL® 718. During a severe accident, the temperature of these materials increase. Interactions between these materials (i.e. eutectic formation, dissolution) may occur during a severe accident. In general, these materials interactions play a significant role in the core degradation and general progression of a severe accident.

A series of simple tests were conducted to examine potential interactions between materials that could occur during a severe accident. This section describes the test setup and results.

3.1 TEST SETUP AND CONDUCT

The same high temperature furnace used for the oxidations tests was used for the materials interaction tests. A small alumina crucible is suspended in the furnace. The crucible has small holes drilled through the lower section sides to allow minor gas flow by the test materials. The two materials to be tested are placed on top of one another inside the crucible and an alumina weight is placed on top. The FeCrAl material was on the bottom for all the tests. The alumina weight ensure the samples remain in contact during the test. The FeCrAl material compisition was Fe-13Cr-6.2Al-0.03Y, with less than 0.01 C and 0.001% sulfur. The metal specimens were lightly polished and not pre-oxidized. The B₄C material had a 99.5% purity (metals basis) and was sourced from Alfa Aesar.

During the test, the furnace is ramped up to the target temperature, held there for 1 hour, and then cooled back down. During this entire time, the furnace is inerted by a flow of argon.

After the test, the samples are removed and photographed. Beyond visual evidence, an indication of whether the two samples interacted is by try to separate them from one another (i.e. manually picking up the top sample off of the bottom sample).

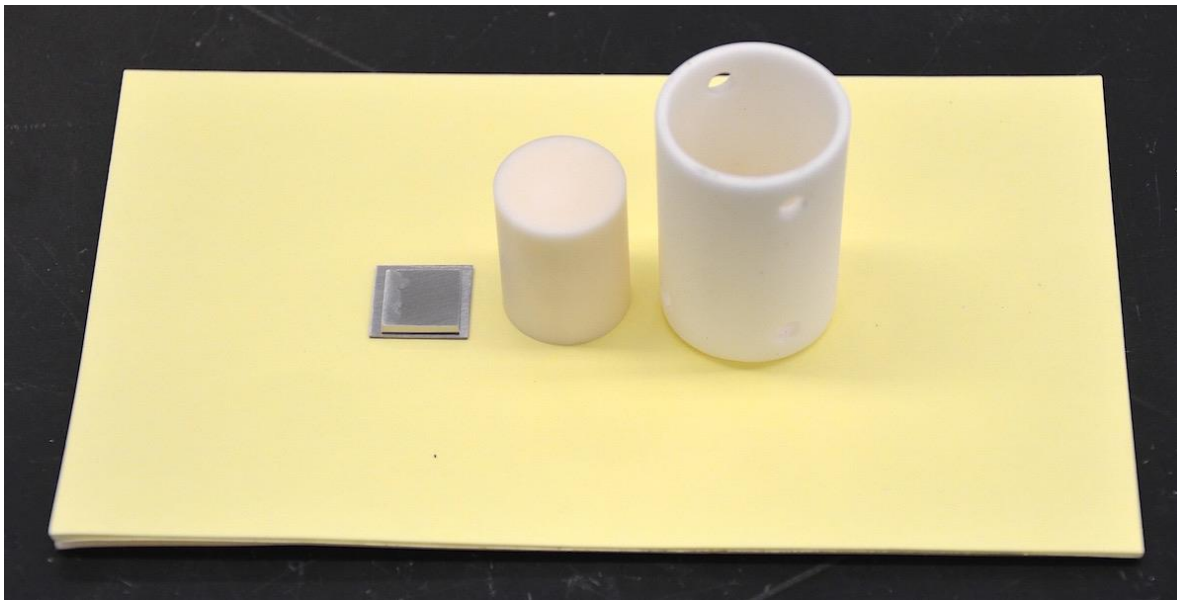


Figure 12. Material interaction test setup.

3.2 TEST SERIES AND RESULTS

The test matrix of material pairings and test temperatures are provided in Table 9. The results of the tests are provided in Table 10 and shown in Table 11. The tests conducted with FeCrAl paired with SS304H, Inconel® 718, or B₄C did not show signs of interaction for test temperatures up to 1450°C. The FeCrAl-B₄C test conducted at 1500°C did appear to have some melting of the FeCrAl; however, the alumina pin suspending the crucible broke during the test and the crucible fell. This test will be repeated in the future.

Table 9. Materials interaction test matrix

Material on bottom	Material on top	Test Number at Test Temperature (°C)			
		1300	1400	1450	1500
FeCrAl	SS304H	3	1		
FeCrAl	Inconel® 718	4	2		
FeCrAl	B ₄ C	6	5	7	8
SS304H	B ₄ C	9			

Table 10. Materials interaction test results

Material on bottom	Material on top	Test Temperature (°C)			
		1300	1400	1450	1500
FeCrAl	SS304H	✓	-		
FeCrAl	Inconel® 718	-	-		
FeCrAl	B ₄ C	✓	✓	✓	X ^a
SS304H	B ₄ C	X			

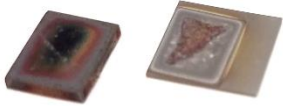
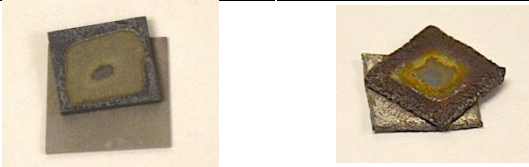


✓ = Materials freely came apart

- = Limited material interaction observed (adhered)

X = More extensive interaction observed melted or dissolution

^a Crucible fell during test, test needs repeated

Table 11. Pictures of materials interaction test results

Material on bottom	Material on top	Test Temperature (°C)		
		1300	1400	1500
FeCrAl	SS304H			
FeCrAl	Inconel® 718			
FeCrAl	B ₄ C			
SS304H	B ₄ C			

Note, the FeCrAl-B₄C at 1450°C is not shown in table.

3.3 RESULTS DISCUSSION

The results with FeCrAl-B₄C are interesting in that Fe-B₄C is known to form a low melting eutectic at approximately 1150°C. In contrast to FeCrAl, the test with SS304H-B₄C exhibited the expected behavior at high temperatures. It is postulated that a thin oxide layer is protecting the FeCrAl material from the B₄C. Future cross-sectional micrographs of the test specimens would likely provide additional insight.

Sakamoto, et. al. [11, 12] conducted a similar series of tests in which two materials in contact were heated to a specified temperature, held at the temperature for one hour all while under an inert atmosphere. Their test matrix and results are summarized in Table 12. The results of the their two FeCrAl-ODS – B₄C tests and the SS316L-B₄C test is corroborated by our recent tests. Their results show FeCrAl maintains compatibility with various materials to higher temperatures than both Zircaloy-4 and SS316L.

Table 12. Materials interaction results of Sakamoto et al [11, 12]

Material on bottom	Material on top	Test Temperature (°C)	
		1300	1400
FeCrAl-ODS	UO ₂		✓[11]
FeCrAl-ODS	B ₄ C	✓[12]	✓[11]
FeCrAl-ODS	Zircaloy-4	- [12]	
UO ₂	Zircaloy-4		- [11]
SS316L	Zircaloy-4	X[12]	
SS316L	B ₄ C	X[12]	

✓ = Materials interaction was noted not to occur

- = Limited material interaction observed

X = Some evidence of materials interaction

4. SUMMARY

FeCrAl alloys are under active development as an ATF concept. The concept's key advantage over Zircaloy is its substantially slower oxidation kinetics up to 1,773 K (1,500°C). To support further development and future adoption, there is a need to assess the potential gains afforded by the FeCrAl ATF concept.

To assess the performance of the FeCrAl ATF concept under severe accident conditions, knowledge of a range of thermophysical and degradation characteristics is needed. Some properties, such as oxidation kinetics, can vary among FeCrAl alloys. The oxidation kinetics of the FeCrAl B136Y (Fe-13Cr-6Al wt %) alloy were investigated using the high-temperature furnace at ORNL. Nineteen segments of B136Y tubing were exposed to a flowing steam environment (~1 atm and 45–55 cm/s) while the system temperature was controlled.

In preparation for a planned QUENCH test using FeCrAl at KIT, one set of oxidation tests were conducted following the planned test temperature sequence. This includes holding the sample at 1,200°C for ~50 min. The test results indicate the B136Y cladding will remain intact for the anticipated peak temperatures of 1,375–1,400°C in the planned FeCrAl QUENCH test. For tests conducted to temperatures of 1,475°C and 1,500°C, the cladding suffered from extensive attack by the steam. In contrast, a second set of tests followed simplified temperature histories based on previously simulated SBO accident scenarios. The B136Y cladding, following more prototypic temperature histories, did not suffer from extensive attack during three tests conducted to 1,500°C.

Based on cladding sample surface area and pre- and posttest mass measurements, the amount of oxidation was determined for the tests. The parabolic oxidation kinetics for the APMT FeCrAl alloy underpredicted the amount of oxidation for the B136Y tubing for the samples not suffering from extensive attack. Although there was scatter in the data, increasing the APMT rate constant by a factor of 5 best reproduced the data set with respect to RMSD. The SBO tests conducted to 1,500°C were best reproduced by increasing the rate constant by a factor of 3.

During a severe accident, materials interactions (e.g. eutectic formation and material dissolution) may occur between the range of materials comprising the reactor core. Interactions between FeCrAl and SS304H, Inconel®718, and B₄C were investigated experimentally in an inert environment. At temperatures below 1500°C, no substantial materials interaction was observed to occur. In contrast, at 1300°C, extensive interaction between SS304H and B₄C was observed. These results are largely consistent with similar tests conducted internationally.

A need continues for additional information on the high-temperature degradation characteristics of FeCrAl cladding and channel boxes. Although a range of test data is available for Zircaloy fuel bundles [10], much accident behavior data is absent for FeCrAl. Tests such as those conducted at the QUENCH facility are needed. Additional needed information includes the possible eutectics formed during degradation, the failure points of the oxides under prototypic conditions, and the relocation characteristics of the collapsed fuel rods. In addition to in-vessel characteristics, further analysis is needed in the behavior of FeCrAl during the ex-vessel portion of the accident progression with respect to molten core-concrete interactions and the possibility for fuel-coolant interactions. Finally, a fuel assembly design has to be developed and analyzed that accounts for thermal-hydraulic, neutronic, fuel, and accident performance, as well as economic considerations.

Notwithstanding future work, the current test results continue to suggest that the FeCrAl ATF concept would provide enhanced accident tolerance for a BWR during SBO severe accidents.

5. REFERENCES

1. F. Goldner, "Development Strategy for Advanced LWR Fuels with Enhanced Accident Tolerance," Enhanced Accident Tolerant LWR Fuels National Metrics Workshop, Germantown, MD, USA, October 2012.
2. K. A. Terrani, S. J. Zinkle, and L. L. Snead, "Advanced Oxidation Resistant Iron-Based Alloys for LWR Fuel Cladding," *J. Nuc. Mat.* 448(1–3), pp. 420–435 (2014).
3. K. R. Robb, M. Howell, L. J. Ott, "Parametric and experimentally informed BWR Severe Accident Analysis Utilizing FeCrAl - M3FT-17OR020205041," ORNL/SPR-2017/373, August 2017.
4. B. A. Pint, K. A. Terrani, M. P. Brady, T. Cheng, and J. R. Keiser, "High temperature oxidation of fuel cladding candidate materials in steam-hydrogen environments," *J. Nuc. Mat.*, 440, pp.420–427 (2013).
5. K. A. Terrani, B. A. Pint, L. L. Snead, and Y. Yamamoto, "High-Temperature Steam Oxidation of Accident Tolerant Fuel Cladding Candidate materials," Proc. of a Technical Meeting Held at ORNL, IAEA-TECDOC-1797, USA, Oct 13–16, 2014.
6. J. Stuckert, M. Große, U. Stegmaier, and M. Steinbrück, *Results of Severe Fuel Damage Experiment QUENCH-15 with ZIRLOTM Cladding Tubes*, Karlsruhe Institute of Technology, KIT-SR 7576, 2011.
7. K. R. Robb, J. W. McMurray, and K. A. Terrani, *M2FT-16OR020205042: Severe Accident Analysis of BWR Core Fueled with UO₂/FeCrAl with Updated Materials and Melt Properties from Experiments*, ORNL/TM-2016/237, Oak Ridge National Laboratory, Oak Ridge, TN, USA, June 2016.
8. Sandia National Laboratories, *MELCOR Computer Code Manuals*, Version 1.8.6, NUREG/CR-6119, Rev. 3, Sandia National Laboratories, Albuquerque, NM, USA, September 2005.
9. B. A. Pint, "Performance of FeCrAl for Accident-Tolerant Fuel Cladding in High Temperature Steam," *Corrosion Reviews*, 35 (2017).
10. J. Rempe, M. Farmer, M. Corradini, L. Ott, R. Gauntt, and D. Powers, "Revisiting Insights from Three Mile Island Unit 2 Postaccident Examinations and Evaluations in View of the Fukushima Daiichi Accident," *J. Nuc. Sci. and Eng.* 172, pp. 223–248 (2012).
11. K. Sakamoto, et al. - Development of Ce-type FeCrAl-ODS ferritic steel to accident tolerant fuel for BWRs - Proc. of TopFuel 2016, Boise, ID, USA, Sept. 11-15, 2016.
12. K. Sakamoto, et al., "A Preliminary Assessment of Applicability of Ferritic ODS Fe-Cr-Al Alloy to Accident Tolerant Fuel and Control Rod for LWRS" Proc. of TopFuel 2015, Zurich, Switzerland, Sept. 13-17, 2015.

APPENDIX A: B136Y OXIDATION TEST DATA

Table A-1. Oxidation test conditions summary

		Segment 1				Segment 2				Segment 3				Segment 4
Test	ID	Temp. (°C)	Ramp Rate (°C/min)	Ramp Time (min)	Hold (min)	Temp. (°C)	Ramp Rate (°C/min)	Ramp Time (min)	Hold (min)	Temp. (°C)	Ramp Rate (°C/min)	Ramp Time (min)	Hold (min)	
1	B136Y312H1m.13615	600	20	30	1	1200	12.00	50	1	STOP				
2	B136Y312H50m.13634	600	20	30	1	1200	12.00	50	50.3	STOP				
3	B136Y314H1m.13650	600	20	30	1	1200	12.00	50	50.3	1400	11.1	18	1	STOP
4	B136Y315H1m.13655	600	20	30	1	1200	12.00	50	50.3	1500	11.1	27	1	STOP
7	B136Y324H1m.13615	600	20	30	1	1412	16.67	48.7	1	STOP				
8	B136Y325H1m.13694	600	20	30	1	1412	16.67	48.7	1	1500	4.17	21.1	1	STOP
9	B136Y322H1m.13695	600	20	30	1	1182	7.41	78.6	1	STOP				
10	B136Y325H1m.13696	600	20	30	1	1182	7.41	78.6	1	1500	1.81	175.5	1	STOP
11	B136Y321H1m.13697	600	20	30	1	1108	5.70	89.2	1	STOP				
12	B136Y325H1m.13709	600	20	30	1	1108	5.70	89.2	1	1500	1.57	249.4	1	STOP
15	B136Y3245H1m.13734	600	20	30	1	1200	12.00	50	50.3	1450	11.1	22.5	1	STOP
16	B136Y3247H1m.13742	600	20	30	1	1200	12.00	50	50.3	1475	11.1	24.8	1	STOP
17	B136Y3255H1m.13663	600	20	30	1	1182	7.41	78.6	1	1550	1.81	203.3	1	STOP
18	B136Y322H1min.13827	600	20	30	1	1200	12.00	50	150.9	STOP				
19	B136Y324H1min.13828	600	20	30	1	1200	12.00	50	50.3	1400	11.1	18	1	STOP
20	B136Y324H1min.14654	600	20	30	1	1200	12.00	50	50.3	1400	11.1	18	1	STOP
21	B136Y322H151min.14659	600	20	30	1	1200	12.00	50	150.9	STOP				
22	B136Y320H1min.14668	600	20	30	1	1050	12.00	37.5	1	STOP				
23	B136Y3255H1min.14669	600	20	30	1	1182	7.41	78.6	1	1550	1.81	203.3	1	STOP

Table A-2. Oxidation test results summary

Test	ID	Dimensions			Initial Wt.	Final Wt.	Wt. Chg.	Area	SMG
		Outer Dia. (mm)	Length (mm)	Thickness (mm)	(mg)	(mg)	(mg)	(cm ²)	(mg/cm ²)
1	B136Y312H1m.13439	9.51	12.63	0.36	972.58	974.14	1.56	7.468	0.21
2	B136Y312H50m.13634	9.51	12.62	0.39	975.77	977.59	1.82	7.455	0.24
3	B136Y314H1m.13650	9.52	12.62	0.39	974.7	981.3	6.60	7.463	0.88
4	B136Y315H1m.13655	9.52	12.62	0.39	974.94	1439.62	464.68	7.463	62.26
7	B136Y324H1.13615	9.51	12.60	0.39	973.63	976.67	3.04	7.444	0.41
8	B136Y325H1m.13694	9.51	12.60	0.40	973.92	979.41	5.49	7.441	0.74
9	B136Y322H1m.13695	9.51	12.61	0.38	973.53	974.6	1.07	7.452	0.14
10	B136Y325H1m.13696	9.51	12.60	0.38	972.01	979.34	7.33	7.446	0.98
11	B136Y321H1m.13697	9.5	12.62	0.39	973.41	975.31	1.9	7.447	0.26
12	B136Y325H1m.13709	9.5	12.6	0.39	973.95	981.49	7.54	7.435	1.01
15	B136Y3245H1m.13734	9.51	12.61	0.39	975.25	979.26	4.01	7.449	0.54
16	B136Y3247H1m.13742	9.51	12.63	0.41	974.69	1416.97	442.28	7.456	59.32
17	B136Y3255H1m.13663	9.51	12.6	0.37	973.35	972.95	-0.4	7.448	-0.05
18	B136Y322H1min.13827	9.51	12.59	0.38	971.09	973.98	2.89	7.44	0.39
19	B136Y324H1min.13828	9.51	15.02	0.39	1155.21	1168.17	12.96	8.83	1.47
20	B136Y324H1min.14654	9.51	12.63	0.37	961.55	966.93	5.38	7.466	0.721
21	B136Y322H151min.14659	9.51	11.97	0.38	921.97	926.67	4.70	7.085	0.663
22	B136Y320H1min.14668	9.51	12.59	0.39	970.27	973.25	2.98	7.438	0.401
23	B136Y3255H1min.14669	9.51	12.63	0.38	14281.83	15130.78	848.95	7.463	113.75